A Hybrid Brain-Computer Interface Fusing P300 ERP and Electrooculography

João Perdiz[1], Aniana Cruz[1], Urbano J. Nunes[1,2] and Gabriel Pires[1,3]

[1] Institute of Systems and Robotics, University of Coimbra, Coimbra, Portugal
joao_perdiz@isr.uc.pt
[2] Department of Electrical and Computer Engineering, University of Coimbra, Coimbra, Portugal
[3] Engineering Department, Polytechnic Institute of Tomar, Tomar, Portugal

Abstract. An Electrooculography-based method is used to correct misclassification of P300 event related potentials in a Lateral Character Speller (LSC) Brain-Computer Interface (BCI). The LSC speller's circular layout allows us to combine P300 detection with the detection of eye movements to improve symbol detection reliability. We separately classify the vertical and horizontal components of Electrooculography signals from shifts in user gaze during intertrial intervals, determining the quadrant of the character the participant will focus on in the next trial. A P300 EEG-based classification decision can then be corrected using quadrant information, selecting the character with the highest probability on that quadrant. This paper focuses on the implementation of the EOG quadrant detector. Preliminary results show good lateral identification but a lower selection accuracy. Empirically, it was possible to conclude that a relatively high percentage of P300 classification errors were corrected using lateral information alone, significantly increasing LSC character selection accuracy.

Keywords: Electrooculography, Character Speller, Event-Related Potentials, EEG

1 Introduction

Brain-Computer Interfaces (BCIs) have enabled people with severe motor disabilities to interact with the outside world using only their brain signals [8, 12]. However, BCI systems still face many challenges such as low number of control commands, low classification accuracy and low transfer rates. In order to overcome these issues and to broaden the target population that can benefit from BCIs, hybrid brain-computer interfaces (hBCI) technology combining brain signals with other physiological signals have been proposed in different ways [9, 5], namely: (a) combination of different physiological signals, such as Electroencephalography (EEG) with Electromyography (EMG) [7], EEG with Electrooculography (EOG) [15] or EEG and functional Near Infrared Spectroscopy (fNIRS) [1]; (b) combination of different neural signals, for example, P300 with motor

imagery or with steady state visual evoked potentials (SSVEP) [18]; and (c) combination of different stimulation modalities such as visual and auditory stimuli [3]. Hybrid BCI approaches have been used in many different applications, such as speller system [17], wheelchair control [16], robotic arm control [6], or controlling a personal computer (e.g., select, open, and close a file) [2]; however, it was concluded that most of the hBCIs proposed in more recent years have combined EEG with EOG [5]. For people who still mantain different functionalities, even if residual, hBCIs can be more advantageous than a single-modality BCI, as all their available funcionalities can be used to provide a more reliable BCI output. The majority of motor disabled people are capable of minor eye movements, thus the EEG/EOG-based hybrid BCI systems might be useful for these BCI target users.

In this work, we present a new EEG/EOG-based hybrid BCI system that takes advantage of the layout of the P300 paradigm by integrating the direction of the user's gaze, extracted from the EOG signal, in the P300-based BCI speller. The new method combines the EEG detection methods already in use in our speller [12] with an EOG-based algorithm that assists the EEG-based core method in selecting the letter the user has chosen during the last spelling iteration. Quadrant detection will be useful for correcting LSC P300 detection errors, since that from datasets collected in [4], we concluded that about 60% of the P300 errors the detected target are in a different quadrant, and about 30% of the errors occur on the side opposite from the target.

2 Background

The Lateral Single Character speller (LSC) is a P300-based BCI communication speller developed in our research group [12] and that has already been used in different scenarios, for example, combined with detection of error related potentials (ErrPs) [4]. LSC's paradigm is significantly different from those commonly found in other character spellers. Specifically, instead of presenting characters in a 6×6 matrix, it has a circular and symmetrical arrangement as shown in Fig. 1. It encodes twenty-eight symbols comprising all letters of the alphabet and the 'space' and 'del' keys. These symbols flash individually according to an oddball paradigm with a flash duration of 75 ms and that alternate between the left and right sides of the screen. The number of event repetitions (N_{rep}) is usually adjusted individually according to user's performance achieved in the calibration session to attain a classification accuracy around 90%.

3 Materials and Methods

3.1 Biosignal acquisition and classification framework

EEG and EOG signals are acquired with a g.USBamp bioamplifier. Signal processing and classification, visual stimuli and visual feedback are implemented in a Matlab/Simulink framework as depicted in Fig. 1. EEG signals were recorded

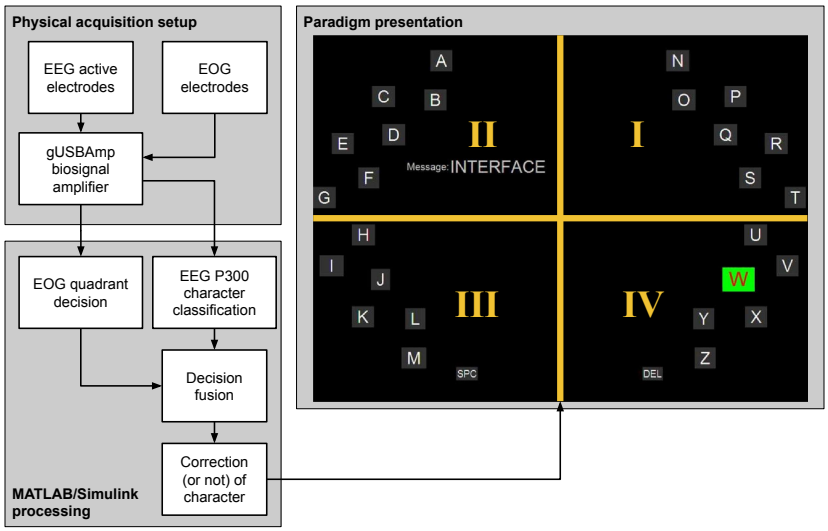

Fig. 1. Physical acquisition setup, classification framework and printscreen of the visual LSC speller [12]. All characters flash for a set number of times, randomly – the highlighted character is flashing green. The message sequence is displayed between the two main groups of characters. Quadrant numbers and divisions shown by yellow markings are not part of the paradigm, but are related to EOG detection.

using 12 electrodes (Fz, Cz, C3, C4, CPz, Pz, P3, P4, PO7, PO8, POz and Oz) placed according to the international extended standard system. The right or left earlobe was used as reference and the AFz electrode was the ground. The EEG signals were filtered using a 1-10Hz bandpass filter and a 50Hz notch filter and sampled at 256Hz.

EOG signals are acquired from a pair of bipolar electrodes in vertical and horizontal layouts around the eyes. They are sampled at 256Hz and filtered with a 50Hz notch filter. Signal sections relevant for quadrant detection are smoothed using a 5th order Savitzky-Golay filter with a frame size of 51 elements.

3.2 Hybrid EEG-EOG paradigm

The LSC letters flash randomly according to an oddball paradigm, thus in each round (flashing sequence) there is one target symbol and 27 standard symbols. Each trial consists of a set of rounds. To select a symbol/letter the user focuses his attention on the target symbol and mentally counts them, ignoring all other standard symbols. The experiment consisted of two phases: calibration and online session. Participants performed the calibration session to gather the EEG data to train the classifier. In this session they had to attend the letters of the sentence "INTERFACES-VISUAIS" which flashed 9 times, gathering 162 target epochs and 4374 non-target epochs. During the online session the partic-

ipants spelled the Portuguese sentence "ESTOU-A-ESCREVER-COM-UMA-INTERFACE-BCI".

The interval between trials (ITI) was set to 4 seconds. During the ITI, just after a trial ends, participants are shown which character was selected by the classification algorithm. They are then required to center their gaze on the cross marking the paradigm's center. After centering the gaze, they choose which character to target next, and then they divert their gaze to the character they want to select. These changes in gaze are monitored using EOG signals, and used to alter the character selection made by the P300 ERP classifier whenever there is a mismatch between the quadrant detected by the EOG detector and the quadrant of the target letter detected with the P300 classifier. The ITI's event progression pipeline is shown in Fig. 2.

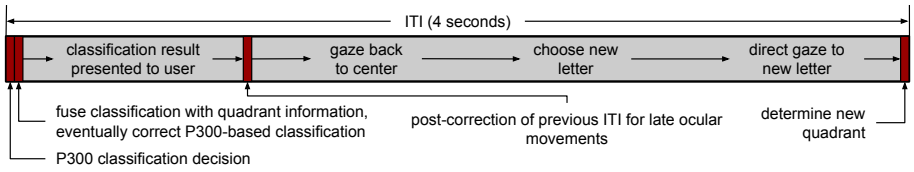

Fig. 2. Sequence of events and processes that occur during an intertrial interval (ITI), from left to right. Shaded sections of the bar show when processing and classification methods are executed, with text indicating the sequence of processes.

Quadrant-based decision correction The combination of horizontal and vertical EOG decisions points us to the quadrant (Q_1, Q_2, Q_3 or Q_4, as shown on Fig. 1) on which gaze is placed before each set of flashing sequences (trial). If this quadrant matches the first choice of the ERP-based classifier in the next trial, no correction is made to the classified character. However, if it conflicts with that outcome, the secondary choice of the ERP classification algorithm is compared and, if matching with the found quadrant, is chosen as the character selected by the user. This method is described more thoroughly in Section 3.5.

3.3 EEG training and classification

Classification of the P300 ERPs is based on a statistical spatial filter called Fisher criterion beamformer (FCB) [11]. EEG data is transformed into projections, from which the two most discriminative projections are classified by a Naive Bayes classifier, which gives a probability (P_s) for each symbol $j = 1, \cdots, N_s$, where $N_s = 28$ is the number of symbols. From this classifier's decision we choose the four symbols with the highest probabilities, according to the rule in Eq. 1:

$$\mathrm{S}_i \equiv \arg\max P_j \quad , j \in \{1, \cdots, N_s\} \backslash \{\emptyset, \cdots, S_{i-1}\}, \quad i \in \{1, 2, 3, 4\} \qquad (1)$$

3.4 Detecting quadrant-related EOG signal changes

The EOG detector detects the quadrant at the end of each ITI, by identifying all the saccades and blinks that occur during that interval. The EOG detector follows an approach similar to that of [10]. However, here, more than one EOG event can occur, since the ITI is much longer than the detection window used in [10]. Moreover, here blinks are undesirable events that need to be eliminated while in [10] they are used as control commands. Blinks are defined as signal peaks, usually detected in vertical EOG, sided by positive and negative first derivative peaks, and exceeding a threshold relative to its neighborhood that is much larger than that used in vertical saccade detection. These characteristics can be seen in Fig. 3. Detected blinks must be at least 0.5s (128 samples) apart. Signal neighborhoods – from both EOG channels – of detected blinks are "flattened" through the use of spline interpolation. All signal points less than 60 samples away from the blink's location are replaced by the interpolation with the rest of each signal's window.

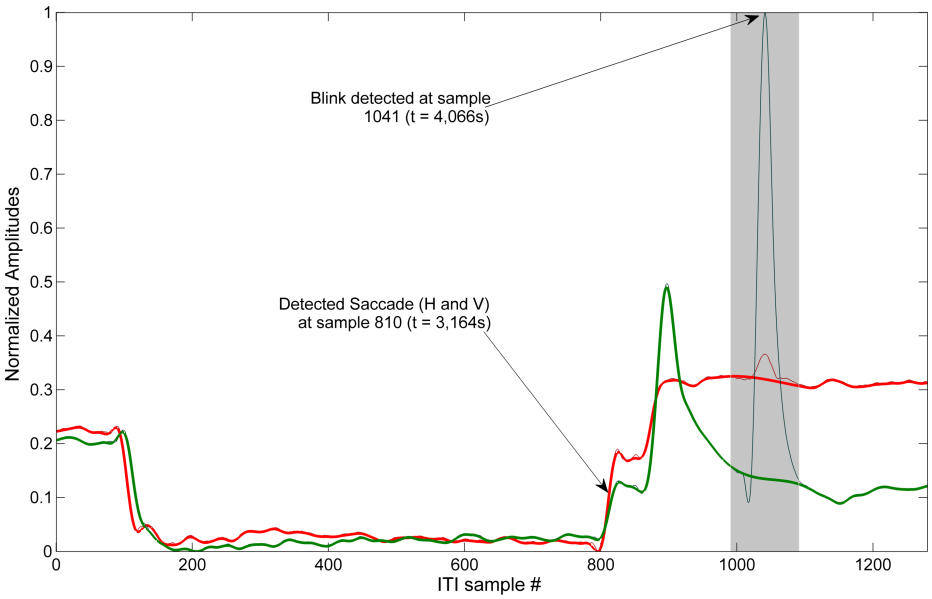

Fig. 3. Typical Horizontal (red) and Vertical (green) EOG signals occurring during one ITI, normalized to the highest amplitude. Thin lines show the signals before smoothing and eliminating blinks. The shaded area shows where each signal was replaced by the spline interpolation of the rest of its window in order to eliminate the blink. Afterwards, horizontal and vertical saccades were found around sample 810.

After blink elimination we search for horizontal saccades. Their clear signature in the horizontal EOG channel is not significantly affected by vertical

components of the ocular movement. Horizontal saccades are identified using the signal's first derivative's peaks, and signal averages before and after these peaks are subtracted and compared to a threshold, meaning that a saccade signal must be step-shaped. We also record the vertical signals for the neighborhoods of valid horizontal events, and locate vertical events in those neighborhoods. Contrary to what happens for horizontal signals, both peaks and steps can be detected in vertical signals. The procedure is described in Algorithm 1.

Moreover, a $1s$ window of the EOG signal (the first second of the previous trial) can be analyzed after the trial ends to detect late ocular events occurring after the end of the ITI; if found, these can affect EOG-based quadrant selection. This post-correction (see Fig. 2) is executed on the ITI following the trial, using the same methods as the main analysis, and may in the same way change the correction issued using the fusion method.

Algorithm 1 Saccade detection algorithm executed upon the horizontal and vertical EOG signal windows during the intertrial interval. The algorithm is applied after the blink elimination algorithm is applied.

Let X_H and X_V be the horizontal and vertical EOG signal during an ITI, splined from raw signals if blinks were previously found; X' denotes a derivative of X
Define horizontal and vertical EOG amplitude thresholds for saccades, Δ_H and Δ_V
Function 1 Find horizontal saccades and record neighborhoods
Find m_p peaks from $|X'_H|$ in locations $p_i : \forall p_i, p_{i+1} - p_i \geq 128 \wedge \forall p_b, p_i - p_b \geq 64$, with p_b marking blink locations
for $m = 1$ **to** $m = m_p$ **do**
  Calculate neighborhood amplitudes before and after peak $p(m)$, $s_{bef} = \overline{X[p(m) - 60, p(m) - 10]}$ and $s_{aft} = \overline{X[p(m) + 10, p(m) + 60]}$
  if $s_{aft} - s_{bef} \geq \Delta_H$ **then**
    Store saccade location $p(m)$, amplitude $a(m)_h = s_{aft} - s_{bef}$, signal $X[p(m) - 127, p(m) + 128]$
  end if
end for

Function 2 Record vertical signals in the neighborhoods of valid horizontal saccades
for $m = 1$ **to** $m = m_p$ **do**
  Find peak location $p_v(m)$ and first derivative peak location $p_{v'}(m)$ of vertical signal in the neighborhood of horizontal saccade in $p(m)$
  if $|p_v(m) - p(m)| \leq 6$ **then**
    Store location $p_v(m)$, signal $X[p_v(m) - 127, p_v(m) + 128]$
  else if $|p_{v'}(m) - p(m)| \leq 6$ **then**
    Store location $p_{v'}(m)$, signal $X[p_{v'}(m) - 127, p_{v'}(m) + 128]$
  end if
end for

Dynamic Time Warping (DTW) is used to calculate the accumulated distances between vertical EOG signals from saccades and six different pre-set functions: a Heaviside, a Logistic, and a Gaussian function, and their y-axis-

inverted variants (Fig. 4), all adapted to 256 samples and normalized to a $[0; 1]$ interval. We model each type of vertical transition as one of these functions, based on the minimization of DTW distance for labelled transitions obtained during calibration.

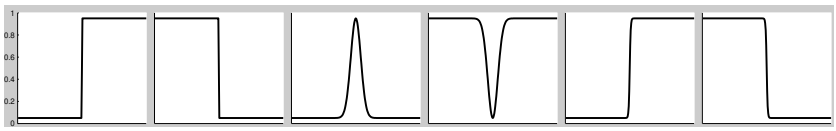

Fig. 4. The six comparison function windows used to train the DTW-based vertical decision method.

After each ITI, a vertical saccade window's DTW distance to each of the model functions is used to classify it as an upward or a downward transition. Horizontal saccades are classified using a linear Bayesian classifier employing horizontal EOG amplitudes as its features. To get the final gaze direction and obtain P_{EOG_H} and P_{EOG_V} for each quadrant (based on vertical EOG scores and horizontal classification probabilities), we only consider the last ocular saccades identified in each direction using the procedure in Algorithm 1.

For each quadrant a gaze probability is calculated as follows:

$$P_{i_{EOG}} = (P_{i_{EOG_H}} \times w_h) \cdot (P_{i_{EOG_V}} \times w_v) \quad , i \in \{Q_1, Q_2, Q_3, Q_4\} \tag{2}$$

Here $P_{i_{EOG_H}}$ only varies between quadrant pairs (1,4) and (2,3), while $P_{i_{EOG_V}}$ varies between pairs (1,2) and (3,4). Weight w_h denotes the weight for the horizontal probability classification, while w_v is the weight for the vertical EOG-based decision. Both are initially set to 0.5.

A diagram of the complete procedure as it integrates into the complete information flow and fusion classification method is shown in the non-shaded area in Fig. 5.

3.5 Fusion of EEG and EOG decisions

The decision of the selected target is based on the weighted fusion of EEG and EOG scores. The latter are obtained through methods described in Section 3.2, while the former are derived from the normalized target ($L_{T_{EEG}}$) and non-target ($L_{nT_{EEG}}$) likelihoods calculated for each character.

This method is a variable-weights fusion method adapted from [14], where weights are updated according to each classifier's agreeance with the fusion final decision. Because EEG-based classification results are not constructed around quadrant information, to convert these results into quadrant information we obtain four graded classification decisions, $S_1 \cdots S_4$, based on Eq. 1.

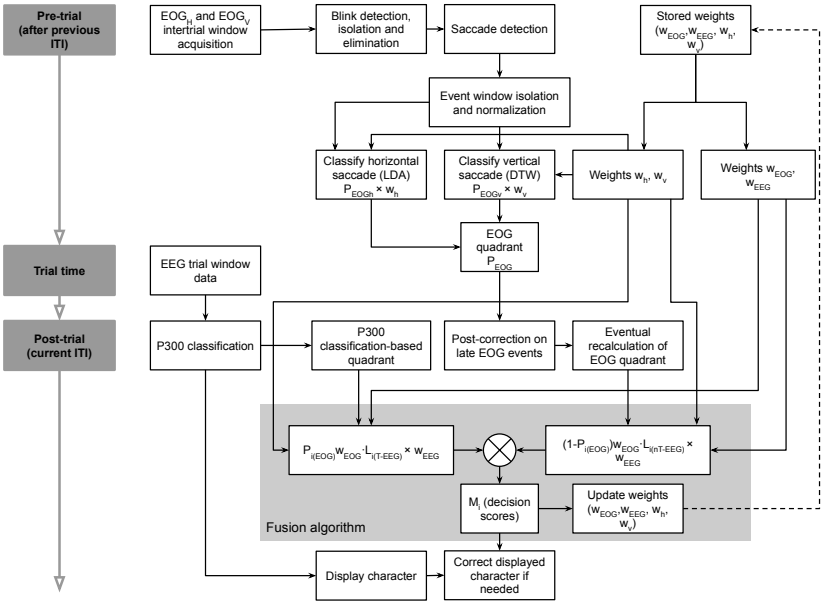

Fig. 5. Full flow diagram of the saccade classification method, the fusion classifier (shaded area), and its influence on character selection on the LSC Speller. Shaded boxes on the left show the stages of the paradigm, and their progression in time. Weights are updated from each fusion branch's success or failure in matching the fusion decision's outcome. Final decision is given by the character that maximizes the vector M of four candidates, chosen through their EEG scores. Dashed lines show weight updates stored for the next ITI.

These four EEG-based decisions form the alternatives that may be chosen when analyzing the EOG events. Their target (T) and non-target (nT) scores are considered and multiplied by EOG-based probabilities and dynamic weights. For every alternative S_n, the $P_{i_{EOG}}$ probability is that of quadrant i where S_n is located.

A final decision vector M is then calculated using the weights attributed to the EEG and EOG signals (Eq. 3), where $w_{EEG} + w_{EOG} = 1$. Final fusion decision is determined from Eq. 4. If the quadrant of the fusion decision is different from the quadrant of the EEG-based character decision, the former replaces the latter as the final character decision for that event, with the weights w_{EEG} and w_{EOG} being updated accordingly.

$$M_i = L_{i_{T_{EEG}}} w_{EEG} \times P_{j_{EOG}} w_{EOG} - L_{i_{nT_{EEG}}} w_{EEG} \times (1 - P_{j_{EOG}}) w_{EOG}, \quad i \in \{Q_1, Q_2, Q_3, Q_4\} \tag{3}$$

$$S_{final} = S_{M_{final}} \quad : \quad M_{final} = \arg\max M_i \tag{4}$$

Weights are updated based on agreeance between signal's decision and the fusion decision. For example, to increment score c_h from Eq. 3, the final fusion decision quadrant and the EOG-determined quadrant must belong to the same side of the speller, i.e. have the same horizontal component. Two pairs of j weights, (w_{EEG}, w_{EOG}) and (w_h, w_v), are updated at event i using the rules in Eq. 5:

$$m_{j_i} = \frac{c_{j_i}}{c_{fusion}}, \quad w_{j_i} = \frac{m_{j_i}}{\sum_{j=1}^{2} m_{j_i}} \tag{5}$$

Here c is a weight-specific success counter updated as shown in Eq. 6, with c_{fusion} serving as the fusion decision's event counter.

$$c_{j_i} = \begin{cases} c_{j_{i-1}} + 1 & \text{if } Q_{signal} = Q_{fusion} \\ c_{j_{i-1}} & \text{if } Q_{signal} \neq Q_{fusion} \end{cases}, \; signal = \{\text{EEG, EOG}\} \tag{6}$$

The full information flow during an intertrial interval and between consecutive intertrial intervals is included in Fig. 5.

4 Results and discussion

In this Section we show the impact of both EOG-based quadrant or side selection on P300-based classification. Table 1 shows the decision accuracies for EOG-based quadrant or side selection for four participants, and the success rate of the vertical EOG component quadrant decision. Quadrant and side selection-based decisions form the basis for Hybrid 1 and Hybrid 2 modes, respectively, whose results are shown further ahead.

From Table 1 we can see that side selection, based on Horizontal EOG, has the highest accuracy. Accuracy of vertical selection is slightly lower than overall quadrant selection accuracy. In Table 2 we show the impact of both EOG components on fusion decision and final character selection accuracy. Here, "Hybrid 1" refers to full quadrant-based weighing of EOG-based decisions and "Hybrid 2" refers to a bilateral, left-right simplified approach.

Table 1. Accuracy of EOG-based quadrant selection and side selection, and vertical component decision. Quadrant selection takes vertical signals into account, while side selection does not.

	EOG Accuracy (%)		
Participant	Quadrant selection	Side selection (L-R)	Up-Down selection
1	86,49	100	84,21
2	89,19	100	86,84
3	86,49	100	84,21
4	56,76	86,49	57,89
Average	**79,73**	**96,62**	**78,29**

Table 2. Register of the accuracies of P-300 based character decisions, on their own and with two different correction modes. Also shown are the percentage of errors corrected (from the EEG classifier) and induced (on the final error count) by each method. The online session consists of 38 events.

	Accuracy (%)			Errors corrected (%)		Errors induced (%)	
Participant	EEG only	Hybrid 1	Hybrid 2	Hybrid 1	Hybrid 2	Hybrid 1	Hybrid 2
1	78,95	86,84	92,11	37,50	62,50	0,00	0,00
2	86,84	84,21	86,84	0,00	0,00	16,67	0,00
3	84,21	92,11	92,11	66,67	66,67	0,00	0,00
4	81,58	78,95	81,58	14,29	28,57	22,22	25,00
Average	**82,90**	**85,53**	**88,16**	**29,62**	**39,43**	**9,72**	**6,25**

Combined with the results shown in Table 1, values in Table 2 confirm that, overall, both of the proposed EOG-based correction modes improve on P300-based character selection accuracy. Also, it can be verified that the vertical channel of EOG has a more important effect in degrading the performance of the EOG-based correction than its horizontal counterpart. On average, the mode without vertical EOG had an additional 2.64 percentage points of accuracy over the quadrant-based method. One of the possible reasons might be the elimination of blinks inadvertently executed during gaze shifts, leading to the exclusion of relevant sections of the signals that cannot then be used to characterize gaze shift. Besides, the participant may be executing the ocular movement towards the next character too late within the ITI, difficulting the acquisition of the relevant signal window on both the horizontal and vertical channels. The impact of this latter issue is larger on vertical signals because of the need for the event to be centered on the window that is inputted to the DTW method. The effects of these issues on vertical accuracy lead us to conclude that the most adequate approach is to only have lateral, left-right-based decisions influencing the P300-based classification.

5 Conclusion

The EOG-based method we have proposed for identifying and correcting errors derived from P300-based classification of EEG signals seems to be valid, with some limitations. We initially envisaged a means to provide quadrant-based information that would be calculated from two channels of EOG signals. However, given the higher error rate of vertical EOG-based decisions, a second method reliant on horizontal EOG was tested and implemented, and found to be better than the quadrant-based process. Lateral identification based on this method has shown very high classification accuracies, which are a prerequisite for identifying errors from P300 given this method's high base accuracy in [4]. Future iterations of the method presented here will require some changes, namely new blink identification procedures able to work in the absence of vertical EOG signals.

Acknowledgments This work was partially funded by the Portuguese Foundation for Science and Technology (FCT) under the Ph.D. Scholarship SFRH/BD/ 104985/2014 of João Perdiz and Ph.D. Scholarship SFRH/BD/ 111473/2015 of Aniana Cruz and was developed at the Institute of Systems and Robotics – University of Coimbra. This work was partially supported by Project B-RELIABLE: SAICT/30935/ 2017, with FEDER/FNR/OE funding through programs CENTRO2020 and FCT, and by UID/EEA/ 00048/2013 with FEDER funding, through programs QREN and COMPETE.

References

1. Ahn, S., Jun, S.C.: Multi-modal integration of EEG-fNIRS for brain-computer interfaces–current limitations and future directions. Frontiers in Human Neuroscience **11** (2017) 503
2. Bai, L., Yu, T., Li, Y.: A brain computer interface-based explorer. Journal of Neuroscience Methods **244** (2015) 2–7
3. Barbosa, S., Pires, G., Nunes, U.: Toward a reliable gaze-independent hybrid BCI combining visual and natural auditory stimuli. Journal of Neuroscience Methods **261** (2016) 47–61
4. Cruz, A., Pires, G., Nunes, U.J.: Double ErrP detection for automatic error correction in an ERP-based BCI speller. IEEE Transactions on Neural Systems and Rehabilitation Engineering **26**(1) (2018) 26–36
5. Hong, K.S., Khan, M.J.: Hybrid brain–computer interface techniques for improved classification accuracy and increased number of commands: a review. Frontiers in Neurorobotics **11** (2017) 35
6. Hortal, E., Iáñez, E., Úbeda, A., Perez-Vidal, C., Azorín, J.M.: Combining a brain–machine interface and an electrooculography interface to perform pick and place tasks with a robotic arm. Robotics and Autonomous Systems **72** (2015) 181–188
7. Leeb, R., Sagha, H., Chavarriaga, R., del R Millán, J.: A hybrid brain–computer interface based on the fusion of electroencephalographic and electromyographic activities. Journal of Neural Engineering **8**(2) (2011) 025011
8. Mak, J.N., Wolpaw, J.R.: Clinical applications of brain-computer interfaces: current state and future prospects. IEEE Reviews in Biomedical Engineering **2** (2009) 187–199
9. Müller-Putz, G., Leeb, R., Tangermann, M., Höhne, J., Kübler, A., Cincotti, F., Mattia, D., Rupp, R., Müller, K.R., Millán, J.d.R.: Towards noninvasive hybrid brain–computer interfaces: framework, practice, clinical application, and beyond. Proceedings of the IEEE **103**(6) (2015) 926–943
10. Perdiz, J., Garrote, L., Pires, G., Nunes, U.J.: Measuring the impact of reinforcement learning on an electrooculography-only computer game. In: 2018 IEEE 6th International Conference on Serious Games and Applications for Health (SeGAH). (May 2018) 1–8
11. Pires, G., Nunes, U., Castelo-Branco, M.: Statistical spatial filtering for a P300-based BCI: tests in able-bodied, and patients with cerebral palsy and amyotrophic lateral sclerosis. Journal of Neuroscience Methods **195**(2) (2011) 270–281
12. Pires, G., Nunes, U., Castelo-Branco, M.: Comparison of a row-column speller vs. a novel lateral single-character speller: assessment of BCI for severe motor disabled patients. Clinical Neurophysiology **123**(6) (2012) 1168–1181

13. Riccio, A., Leotta, F., Bianchi, L., Aloise, F., Zickler, C., Hoogerwerf, E., Kübler, A., Mattia, D., Cincotti, F.: Workload measurement in a communication application operated through a P300-based brain–computer interface. Journal of Neural Engineering **8**(2) (2011) 025028
14. Taher, F.B., Amor, N.B., Jallouli, M.: A multimodal wheelchair control system based on EEG signals and eye tracking fusion. In: 2015 International Symposium on Innovations in Intelligent SysTems and Applications (INISTA), IEEE (2015) 1–8
15. Usakli, A., Gurkan, S., Aloise, F., Vecchiato, G., Babiloni, F.: A hybrid platform based on EOG and EEG signals to restore communication for patients afflicted with progressive motor neuron diseases. In: 2009 Annual International Conference of the IEEE Engineering in Medicine and Biology Society, IEEE (2009) 543–546
16. Wang, H., Li, Y., Long, J., Yu, T., Gu, Z.: An asynchronous wheelchair control by hybrid EEG–EOG brain–computer interface. Cognitive Neurodynamics **8**(5) (2014) 399–409
17. Yin, E., Zeyl, T., Saab, R., Chau, T., Hu, D., Zhou, Z.: A hybrid brain–computer interface based on the fusion of P300 and SSVEP scores. IEEE Transactions on Neural Systems and Rehabilitation Engineering **23**(4) (2015) 693–701
18. Zhang, R., Li, Y., Yan, Y., Zhang, H., Wu, S., Yu, T., Gu, Z.: Control of a wheelchair in an indoor environment based on a brain–computer interface and automated navigation. IEEE Transactions on Neural Systems and Rehabilitation Engineering **24**(1) (2016) 128–139